Surface Science 94 (1980) 1–15

THERMAL RESISTIVITY OF LAYERED ^{4}He FILMS ON ZYX GRAPHITE BELOW 2 K

S.E. POLANCO * and Michael BRETZ
Department of Physics, University of Michigan, Ann Arbor, Michigan 48109, USA

Received 25 October 1979; accepted for publication 27 December 1979

Thermal resistance and vapor pressure isotherms were taken near superfluid onset for ultra-thin helium films adsorbed on a ZYX graphite wafer between 1–2 K and 3–7 atomic layers. Our data are consistent with previous graphite onsets and are compatible with a current model of film droplet formation. Overlap of thermal resistance curves at 1.19 and 139 K is believed to be associated with discrete layering effects of 2D superfluid film properties.

1. Background

Several techniques – thermal conductivity and mass flow [1], third sound [2], persistent currents [3], quartz microbalance [4] – have been used to explore superfluid properties for ultra-thin films adsorbed on glass, rutile, quartz, etc. Complementing these multilayer experiments on heterogeneous substrates, investigations have been made for multilayer helium films adsorbed on Grafoil [5], a relatively homogeneous surface for physical adsorption. Of particular interest are the characteristic differences in vapor pressure isotherms, specific heat, and superfluid onset which were noted for these two classes of substrates [6]. Recently researchers have been deliberating on whether the 2D superfluid properties theorized by Kosterlitz, Thouless and Nelson [7] have been achieved experimentally. Torsional pendulum measurements of Bishop and Reppy [8] for helium on Mylar and reanalysis of 3rd sound data on glass by Rudnick [9] are consistent with these expectations. However, Dash [10] points out that superfluid onsets within a single atomic layer may be influenced by the presence of other 2D film phases which are known to exist [11]. Moreover, Huberman and Dash [12] argue that multilayer films probably involve 3D droplet condensation and associated Josephson tunneling which would make the analysis of superfluid onset more complex than can be accommodated by the present 2D onset theory. This paper adds weight to the arguments for including droplets and also film layering in further analyses.

* Present address: Bell Telephone Laboratories, Allentown, Pennsylvania 18103, USA.

2. The experiment

2.1. Apparatus

We report a thermal resistance exploration of the transition region from ultra-thin liquid to discretely layered films [13]. UCAR-ZYX graphite [5], used in the present study, has already been shown to enhance monolayer phase transitions [14, 15] and to allow the formation of about 5 discrete helium layers [16]. Our thermal resistance cell shown in fig. 1, contains a single, cleaned (at 1000°C in vacuum), 1 X 1 X 3/16 inch wafer of ZYZ press-fitted into a thin walled (0.59 mm) stainless box having copper end-plates (cell dead volume is 1.16 cm^3). One end was mounted directly to the pot of a ^{3}He cryostat while the other end, containing a heater, remained thermally isolated. Two thin-slab carbon thermometers W and C (470 Ω Speer resistors ground to 1 mm thickness) were varnished in place near the cell ends with thermometer C used to regulate the ^{3}He pot at a constant temperature. This configuration minimized end-plate boundary resistance problems in this steady state experiment since the heat $\dot{Q}$ flows past C and W on its way from heater to ^{3}He reservoir. Differential contraction within the cell was considered acceptable as the basal plane of graphite expands when cooled and exfoliated crystals possess their own spring action along the c-axis [17]. The cell always contained a finite vapor

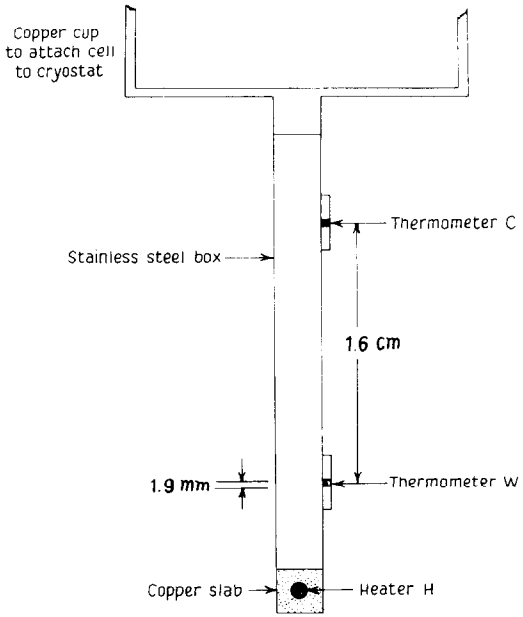

Fig. 1. Schematic diagram of the experimental cell.

pressure which enhances the thermal conductance between stainless walls and ZYX wafer. A limitation of experimental sensitivity arises from the long gas relaxation times of ZYX, which undoubtedly inhibit gas return flow in such a superfluid–vapor heat pipe experiment. On the other hand, the ZYX adsorption chambers are believed to be extensive, which allows heat transfer within each chamber, and heat should travel efficiently along graphite sheets between adjacent adsorption chambers (approximating an array of connected heat pipes).

2.2. Thermal resistivity

The experiment was performed as follows. Steady state temperature differences ΔT maintained across the cell resistors were measured for various heat inputs $\dot{Q}$. Each measurement set comprises one constant coverage curve, several of which are shown in fig. 2 for the cell resistor C regulated at 1.19 K. At low coverages we find a linear dependence of ΔT on $\dot{Q}$ whose slope is the total thermal resistance of the cell. This resistance decreases as the film thickens since there is more liquid to transport the heat. For the highest coverages the linear extra-polations of the data points no longer pass through the origin. We interpret these finite $\dot{Q}$ offsets at $\Delta T = 0$ as evidence of superfluidlike behavior, and take onset to occur between the two ΔT versus $\dot{Q}$ regimes. (These onsets will be represented by asterisks in the subsequent figures.) Actually, our ZYX geometry is too complex to expect a true $\Delta T = 0$ offset. The low $\dot{Q}$ behavior of the fig. 2 inset shows that the constant coverage curves do eventually head linearly for the origin. We believe that the crossover region to low $\dot{Q}$ involves critical velocity effects in the film superfluid. Thus, the low $\dot{Q}$ slopes from the fig. 2 inset are used in further thermal resistance analysis.

The total cell thermal resistance is plotted in fig. 3. Isotherms are presented at five temperatures separated by 0.2 K intervals. As coverage builds the cell slowly decreases in resistance before dropping rapidly toward zero resistance within a region bracketing our superfluid onsets (asterisks). It is evident that an irregularity is present in the onset curves. Instead of onset regions being nicely spaced corresponding to the even temperature intervals of the isotherms, the curves at 1.19 and 1.39 K in fact overlap. This intriguing feature, as well as other film thermal properties, can be viewed more clearly when the empty cell is subtracted from the signal [18]. We show the corrected curves in fig. 4 where the film thermal resistance has been multiplied by coverage to obtain a measure of film resistivity. That is, we are plotting the *average* film resistivity per atomic layer of film, including the 1st and 2nd layer solids (an implicit assumption here is that thickness is proportional to coverage). The overall shapes of the isotherms are similar to those of fig. 3. We have included dotted lines to indicate the maximum extent of systematic errors involved in the vapor corrections which were made. These become vanishingly small at the lower temperatures where the onset irregularity was observed. One can see that the irregularity is still present, even enhanced here, with an almost complete overlap of the 1.19 and 1.39 K isotherms in the transition region. We will analyze

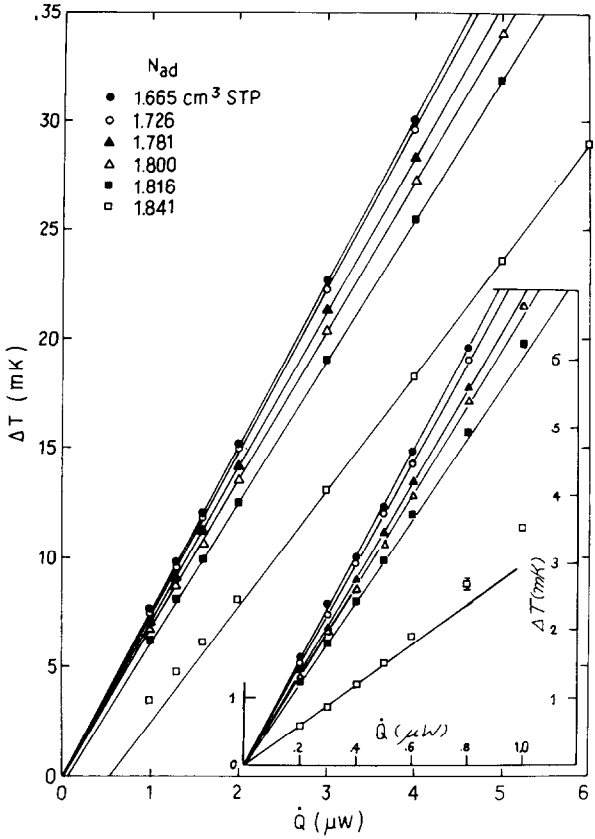

Fig. 2. Cell thermometer difference ΔT versus heat input $\dot{Q}$ at 1.19 K. Insert is data for low heating levels.

this important disruption of the superfluid onset temperature–coverage relation later in the discussion section of the paper. Let us emphasize here, however, that the 1.19 and 1.39 K isotherms were checked and rechecked with great care taken in calculating the error bars in N_{ad}. The data are consistent with the two curves coinciding.

The resistivities of very low coverage films in fig. 4 are observed to increase as the temperature decreases. This trend agrees with the temperature dependence of bulk normal helium. The low coverage data also indicates an increase of resistivity with coverage at constant temperature. This feature is in turn explained by density variations within the film. The first two ^{4}He layers are dense solids with a thermal resistivity about two orders of magnitude smaller than the liquid. Higher layers are less dense, eventuall approaching bulk liquid. Hence the average film resitivity

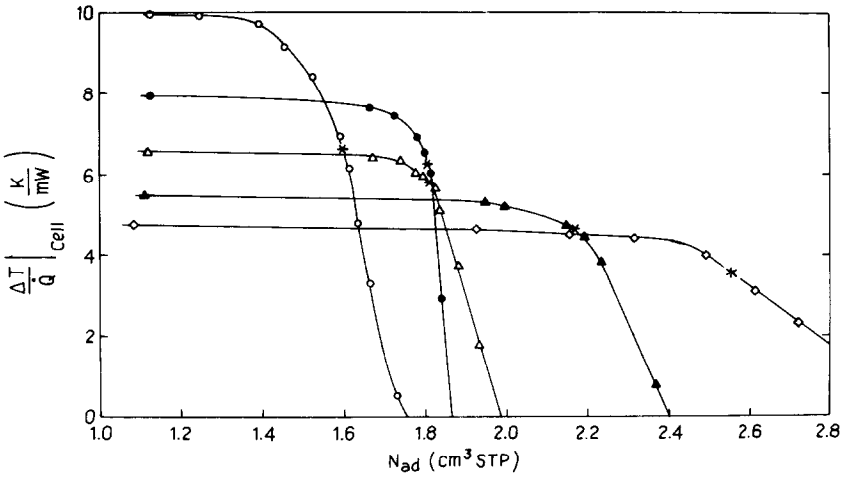

Fig. 3. Total thermal resistance of the cell as a function of film coverage. Lines guide the eye. Symbols correspond to the following temperatures: (○) 1.00 K; (●) 1.19 K; (△) 1.39 K; (▲) 1.60 K; (◇) 1.81 K. Asterisks denote first appearance of superfluidity.

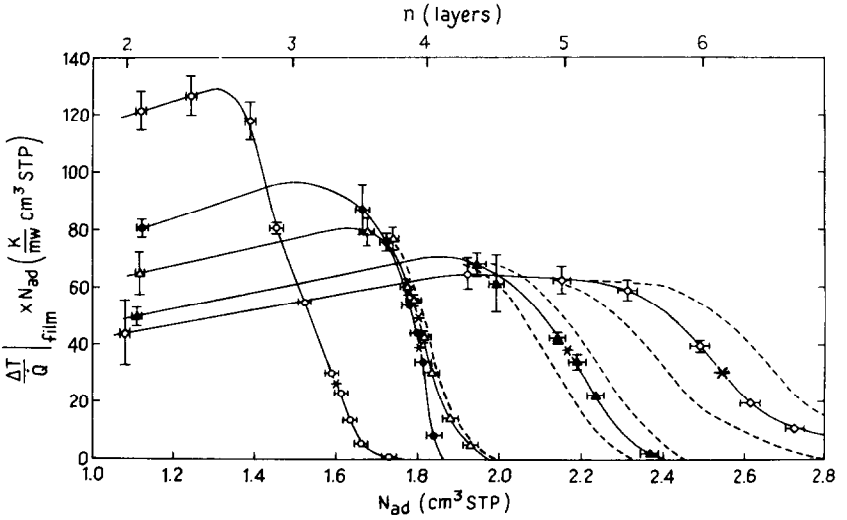

Fig. 4. Normalized film thermal resistivities as a function of gas filling (below) and layer number (above). Symbols are the same as fig. 3. Asterisks denote first appearance of film superfluid. Vertical error bars reflect uncertainties in the determination of slopes from fig. 2 while horizontal error bars show gas metering accuracy. Dashed lines are estimates of systematic errors from vapor in the cell dead volume.

increases as atoms are added to the liquid-like layers. In principle it should be possible to subtract out the thermal resistivity of the solid layers. Unfortunately, experimental error in the measurement of the second layer thermal resistance was too large for a meaningful subtraction to be performed.

All thermal resistance isotherms of fig. 4 have temperature dependent high coverage tails. Two possible mechanisms for the origin of tails are wafer-wall contact resistance variations and return gas flow impedance problems within the interconnected XYX voids. However, impedances due to these processes alone would diminish rather than grow with increasing temperature since both thermal contact conductance and mass flow improve with temperature. Therefore, there must be at least one additional impedance to heat transfer within the helium–graphite system.

2.3. Isotherms

The cell vapor pressure was monitored continuously as it was needed for coverage determinations. Since the pressure data are not in a form amenable to interpretation, separate ^{4}He vapor pressure isotherms at 2.0 K and near 1.37 K were subsequently measured (see fig. 5). The 1.35–1.40 K isotherms were taken with the cell attached to a different cryostat of somewhat poorer design. Thus, small variations in absolute coverage and temperature calibration are of comparable size to the expected temperature dependent offset of μ/kT for the various isotherms, where μ is the system chemical potential. For this reason, data at 1.35 and 1.40 K were shifted vertically by a few percent to provide a smooth continuation with the 1.37 K points. (These points still retain the linear T dependence already incorporated in the ordinate scale). The conversion to μ was made using

$$\mu = kT \ln \left| \frac{\lambda^3 P}{kT} \right| ,$$

where

$$\lambda = h/(2\pi mkT)^{1/2}$$

is the atomic thermal wavelength. Straight line segments were drawn through the data for each of the 1.37 K isotherm plateaus. (As expected, the 1.37 K isotherm features are more distinct than those for the 2 K isotherm.) Consistent with an earlier analysis [11], we took the isotherm breakaway from these lines as signaling layer completion. The conversion from cm^3 STP to layer number was then constructed and appears on the scale of fig. 4. The 4th layer contains about 0.35 cm^3 STP and the 3rd layer 0.4 cm^3 STP, with 1.07 cm^3 STP remaining for the 2nd and 1st layer solids. Assuming monolayer capacity to be 0.63 ccSTP gives layer capacity ratios of 1/0.70/0.64/0.56 for the 1st to 4th layers, which is in fair agreement with the original helium on Grafoil multilayer determination of 1.0/0.71/0.67/0.67/... obtained from a combination of heat capacity and Frenkel–Halsey–Hill isotherm

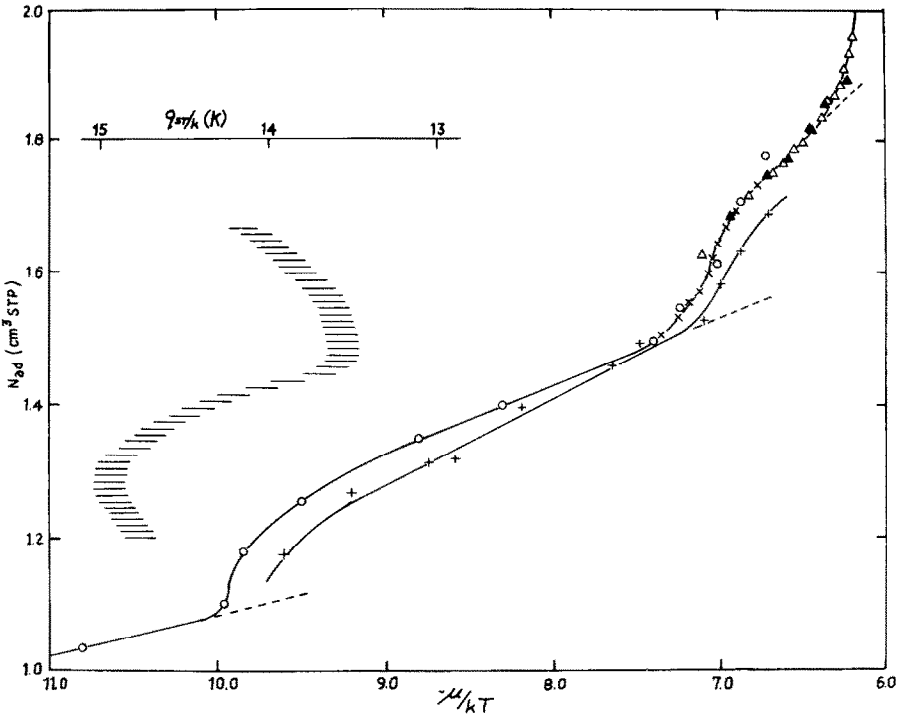

Fig. 5. ^{4}He system chemical potentials and resulting isosteric heat of adsorption $q_{st/k}$ for 1.69 K. Symbols are: (+) 2.0 K; (○) 1.40 K; (×) 1.37 K; (△) 1.35 K. Solid lines guide the eye. For comparison the 2 K isotherm is shifted left by 2 units in μ/kT.

analysis [19]. Values are somewhat lower than the previous ZYX multilayer determination from a combined desorption heat capacity peak and vapor pressure analysis [16]. That calibration covered a range of temperatures and relied on a comparison between different ZYX cells. The present calibration from the fig. 5 breakaway coverages is superior and thus supersedes the earlier determination.

We have calculated an approximate isosteric heat of adsorption, q_{st}, over a narrow coverage range using the thermodynamic relation

$$\frac{q_{st}}{k} = kT^2 \left| \frac{\partial \ln P}{\partial T} \right|_{N_{ad}} = \tfrac{5}{2}T + T^2 \left| \frac{\partial(\mu/T)}{\partial T} \right|_{N_{ad}}, \tag{1}$$

and the combined fig. 5 isotherms. The shape of q_{st}/k, sketched in fig. 5, agrees with the more complete curve found in ref. [16] (which unfortunately appears to possess a scale error). The heat of adsorption for bulk helium, 10.5 K, is a few degrees less than the q_{st} range for the 3–4 layer films.

3. Discussion

3.1. Comparison of ZYX onsets to previous experiments

Values of P_c/P_0 versus T_c are plotted in fig. 6a for several superfluid onset experiments, where T_c and P_c are the transition temperature and pressure of the unsaturated film and P_0 is the vapor pressure of bulk at T_c. The data on heterogeneous substrates lie around the solid line in fig. 6a. Grafoil thermal onsets [19] are

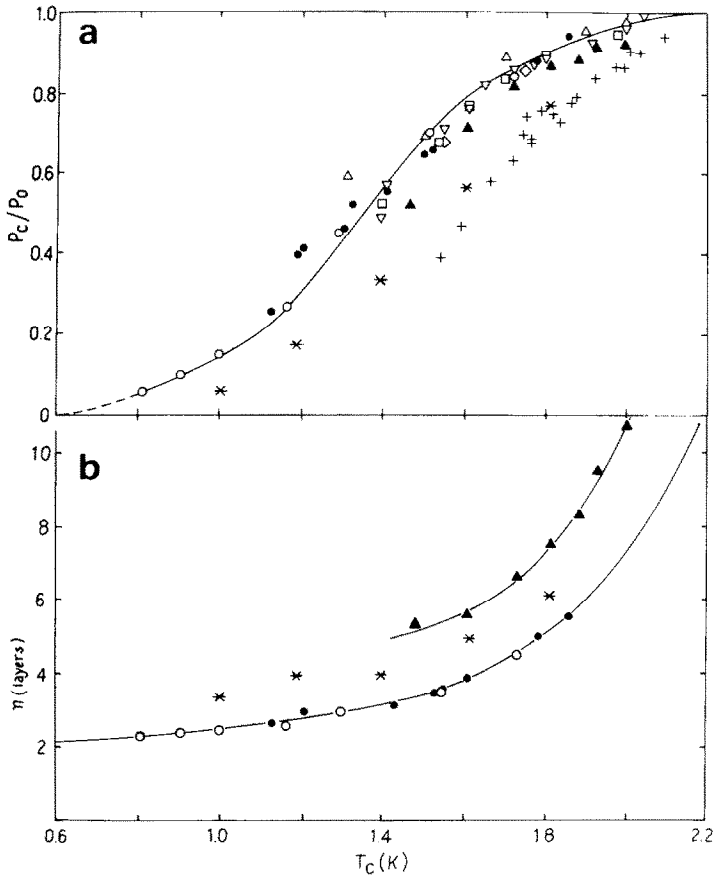

Fig. 6. (a) Onset values P_c/P_0 for different substrates and experimental methods, plotted against onset temperature. Mass transport: (△) Long and Meyer [1]; (+) Herb and Dash [20]. Persistent currents: (◇) Henkel et al. [3]. Third sound: (●) Kagiwada et al. [2]. Thermal transport: (▽) Long and Meyer [1]; (□) Brewer and Mendelssohn [1]; (○) Fokkens et al. [1]; (▲) Bretz [19]; (*) this experiment. (b) Onset temperature T_c versus layer number n_c. (▲) Grafoil [19]; (*) ZYX; (○), (●) glass [1,2]. Solid lines are the linear fits of fig. 7.

also close to this line, but onsets from the mass flow experiments of Herb and Dash [20] are offset by 0.1–0.3 K. Present ZYX results lie between those of the Grafoil experiments but considerably closer to the mass flow data. Since P_c/P_0 is a measure of film thickness, the three graphite experiments seem to yield different onset temperature–thickness relations. This discrepancy arises from the relative sensitivities of the various graphite onset experiments. Bretz [19] chose his Grafoil onsets where the film thermal conductivity became too large to measure. They correspond to vanishing thermal resistances in fig. 4, which occur at larger thicknesses than the asterisks defining onset in this experiment. That Herb's onsets occur for even thinner films simply means that mass flow is a somewhat more sensitive probe of superfluidity than is thermal transport.

Since P_c/P_0 is a catch-all parameter involving thickness, heat of adsorption, condensation effects, etc., we have replotted some of the graphite and glass results as onset layer number n_c versus temperature T_c in fig. 6b. Film thicknesses on glass were determined by direct application of the Frenkel–Halsey–Hill isotherm (FHH) with $\alpha = 27$ layers ^{3}K. Bretz's published Grafoil coverages [19], were corrected from $T = 0$ values to the actual number of atoms in the film at onset. ZYX film thicknesses were determined by measuring the gas admitted to the cell, and after vapor corrections, compared to the layer capacities obtained in fig. 5. (It was not possible to accurately convert Herb and Dash's mass flow P_c/P_0 values to layer number for fig. 6b.) We point out that although FHH analyses were used for ^{4}He films on both glass and Grafoil, the results are not firm. Vidali, Cole and Schwartz [21] report that adsorption potentials of helium on graphite are not well established. And although Sabisky and Anderson [22] find excellent agreement between their acoustic measurements and the FHH prediction on a number of substrates, their analysis is subject to sizable coverage shifts.

It is tempting to say that the P_c/P_0 versus plot of fig. 6a implies superfluid onset at a given temperature occurs in *thinner* films on graphite. That statement is incorrect because it neglects large differences in the value of α from one substrate to another. It is seen in fig. 6b that film thickness at onset appears *larger* on graphite than on glass. In fact, the n_c versus T_c curve for graphite parallels that of glass, displaced by about 1 layer for ZYX and 2 layers for Grafoil. (In view of our agreement with Herb and Dash, we give considerably more weight to the ZYX vis-à-vis the Grafoil specific heat/thermal onset data.) This similarity of shape is interpreted as meaning that glass and graphite have similar effects on film superfluidity with the displacement reflecting a thicker inert layer for the stronger adsorbent. But due to our uncertainty of absolute coverage on glass, the possibility remains that onsets are identical for ZYX and glass surfaces even though α is much larger on graphite.

3.2. Droplet nucleation model

As mentioned in the introduction, the Huberman–Dash model [12] of superfluid percolation through an array of surface droplets was presented as a mecha-

nism of helium film growth and dynamics. In this model bulk droplets are nucleated at surface imperfections on films thicker than a critical thickness n_0, and become superfluid at or near T_λ. Huberman and Dash considered the problem of connectivity between neighboring superfluid droplets. They pointed out that there are weak links via quantum-mechanical leakage through the underlying uniform film. They also suggested that as the temperature is reduced, or coverage increased, the quantum phase angles of the complex order parameter of neighboring droplets become progressively correlated. Superfluid onset takes place when correlations extend over the entire surface. Thus, onset of superflow is a percolation transition of the order parameter phase angles. Huberman and Dash applied the classical, two-dimensional, XY model to this problem, and derived the following relationship between onset thickness n_c and temperature T_c:

$$\frac{T_c}{T_\lambda} = \frac{\exp[-k/(n_c - n_0)^{1/2}]}{\exp[-k/(n_\lambda - n_0)^{1/2}]}. \tag{2}$$

Here n_λ is the coverage at which the onset temperature becomes T_λ, and k is a constant incorporating the density of nucleation sites and the transmission coefficient in the uniform film. This equation assumes that films grow by increasing the number of droplets of nearly constant size, and that droplets become superfluid at T_λ (i.e., no effects of restricted geometry). Fig. 7 compares the Huberman–Dash prediction to the glass and graphite data in fig. 6b. These experiments are appropriate for comparison to a connectivity model because they require transport over macroscopic distances. The large range of temperatures covered by the combined glass data allows determination of the critical thickness n_0 by fitting to the above relation while n_0 is varied. The best fit for glass was obtained for n_0 = 1.8 layers. It

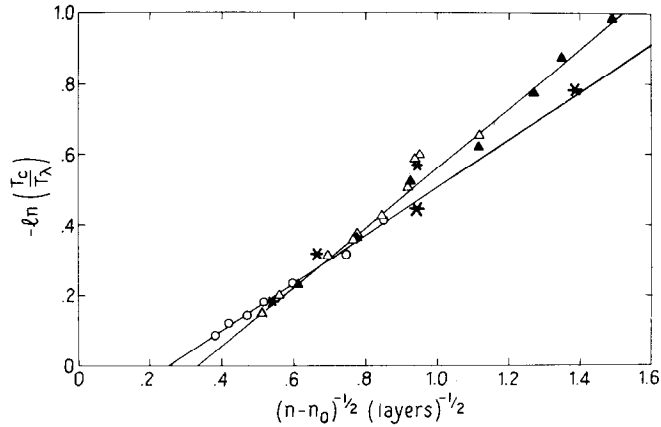

Fig. 7. Comparison of glass and graphite data to the Huberman–Dash theory: (○) Grafoil; (△), (▲) glass; (*) ZYX. Straight line fits for glass, ZYX and Grafoil data with n_0 = 1.8, 2.8 and 3.8 respectively.

is quite good over the whole range of temperatures, supporting the applicability of this model to macroscopic transport experiments. The Grafoil data are not extensive enough for a similar determination of the critical thickness. However, since the onset curves for Grafoil and glass are similar in shape but are displaced on the coverage axis (see fig. 6b), the superfluid transition appears to be the same on both substrates with a thicker underlying film on the stronger adsorbent. The separation of the onset curves is about 2 layers, indicating $n_0 \approx 3.8$ layers on Grafoil. The straight line fit using this n_0 signifies that the Grafoil data are also in good agreement with the Huberman-Dash percolation model. By extrapolation to the horizontal axis, we find thicknesses n for geometric connectivity at 11.3 and 19.8 layers for glass and Grafoil respectively.

The ZYX onsets with $n_0 = 2.8$ layers appears as the asterisks in fig. 7. This value was chosen to reflect the position of the ZYX data between the glass and Grafoil curves of fig. 6b. Although the onset datum at 1.19 K looks anomalous, the other points fall close to the Grafoil fit. The Huberman–Dash ZYX analysis should not be pushed too far since systematic errors grow with coverage (see fig. 4) and because the ZYX n_0 corresponds to onsets occurring in the transition region rather than at full macroscopic connectivity.

The non-uniform film model does agree with other thermal conductivity features which we will now discuss. Below T_λ the film is pictured as consisting of isolated superfluid clusters joined by thinner normal regions. The vanishing thermal resistance of the bulk clusters makes the total film resistance fall below that of a normal film. But this reduction is small when there are only a few unconnected droplets, as any path across the cell will be made up almost entirely of the intervening normal regions. Each isolated drop can conduct with vanishing thermal resistance only the fraction of $\dot{Q}$ which reaches it through the adjacent normal film. This fraction can be so small that the critical heat $\dot{Q}_c$ is not exceeded at the power levels and temperature differences of this experiment. Hence films with a few small droplets have finite thermal resistances, and linear ΔT versus $\dot{Q}$ relationships, even though some superfluid is present. As coverage is increased the superfluid clusters become better connected, conducting a large fraction of $\dot{Q}$. The thermal resistances of these thicker films, while still finite, are much smaller than if they were normal. Their $\dot{Q}_c$'s can be exceeded, and the ΔT versus $\dot{Q}$ plots have the curvature previously associated with superfluidlike behavior (fig. 2). Connectivity increases with increasing coverage, until finally a superfluid path is formed across the length of the film. Then all of $\dot{Q}$ is conducted by the superfluid, and the film exhibits a vanishing thermal resistance. According to this model the asterisks in figs. 3 and 4 mark the coverage where enough connectivity is achieved for $\dot{Q}_c$ to be exceeded. Thus, clustering is not only consistent with the sizable width of the transition region, but with the locations of the asterisks inside the transitions as well. The residual high coverage tails might also originate by a similar percolation process among the various macroscopic graphite crystallites. For analogous effects in granular superconducting thin films, see ref. [23].

The trend of transition width versus thickness is determined by the way in which bulk droplets grow. Films become increasingly more uniform, and onsets narrower, if drops grow mostly in the lateral directions. But the opposite is true if most of the growth is in droplet height. Cole et al. [24] pointed out that thickness variations grow with thickness in films which are thin compared to the typical distance of variations in binding energy. In such films the superfluid transition becomes wider as coverage is increased. However, if a film is thicker than the substrate's lateral scale of heterogeneity, atoms at the top interact with a growing region of substrate material which has an increasingly broad range of binding energies. Then effects of heterogeneity tend to average out, and the superfluid transition becomes sharper as the film becomes more uniform. ZYX graphite is known to be highly homogeneous, and to have a microcrystallite size of several hundred angstroms [14,15]. Although the typical distance of binding energy variations is not known, it is certainly larger than the film thicknesses of this experiment (about 10 to 30 Å). Hence these films are in the region of increasing thickness variations, and the connectivity argument is consistent with the trend in transition widths.

In summary then, we find the Huberman-Dash model of value in understanding various characteristic features of our ZYX data which would otherwise be without explanation. Although our survey of onsets was not extensive enough to do a quantitative analysis for ZYX data, we have shown its consistency with previous work which does seem to agree quantitatively with the proposed film model. The ultimate judgment of that model will certainly be based on a variety of experimental results which will include the present analysis.

3.3. Contiguity of thermal resistance curves at 1.19 and 1.39 K

The most startling result of this experiment is the overlap of the 1.19 and 1.39 thermal resistance curves in fig. 4. Previous onset experiments had not found this feature, which is inconsistent with both the Huberman–Dash theory and models of superfluid onset in uniform films. In particular, the close proximity of these curves disagrees wth the theory of Kosterlitz, Thouless, and Nelson [7] which predicts a smooth thickness temperature relationship at onset as long as the superfluid density is only depleted by vortex-pair breaking. The 1.00 K curve is shifted again to thinner films. Possibly this 1 K transition takes place in a uniform film thinner than the critical thickness above which drops nucleate, where we expect Kosterlitz–Nelson–Thouless theories to be appropriate. This agrees with Dash's estimations, based on both experimental and theoretical arguments, that the critical thickness is 3 or 4 layers [25].

It is possible, but unlikely that this anomaly is an irregularity inherent in the thermal resistance measurement which depends on vapor phase return flow properties. The ZYX void spaces are visualized as long, narrow, flat channels between crystalline graphite leaves. The total adsorption area measured by an argon isotherm [13] at 77 K is 1.20 m^2 giving roughly 2100 exposed basal planes in the 1 × 1 inch

ZYX wafer. Since the cell is approximately 80% dead volume, the average exposed plane separation is about 1.9 μm. Jelatis et al. [26] have emphasized that helium vapor is not in thermodynamic equilibrium when its mean free path, l, is substantially greater than the film separation on two adjacent surfaces. For our film at 1.6 K, l is about 0.2 μm, but l becomes comparable to the *average* void size at 1.39 K ($0.6 \lesssim l \lesssim 1.2$ μm) and becomes significantly larger than the void size at 1.19 K ($3 \lesssim l \lesssim 8$ μm). However, the actual ZYX chambers do not correspond well to the average voids. Since the adsorption chambers narrow down at the edges, even the 1.6 and 1.8 K data have a significant fraction of returning gas atoms in regions with $l \gg$ void size. So as T is lowered, the evolution of the system from $l \ll$ voids to $l \gg$ voids must certainly be a gradual and therefore smooth process. Moreover, the 1 K curve appears well-behaved again, being displaced significantly in coverage from the 1.19 K data. These arguments lead us to believe that mean-free path considerations are insufficient to explain our irregularity in thermal conductivity.

It should be noted that the wafer/cell wall spacing is about the same as the average ZYX void spacing [17] so additional gas flow features will not appear. Also, a glance back at fig. 6a will be sufficient to end concerns of superfluidity on the stainless cell wall. At a given pressure such a film would go normal before the ZYX transition region is entered.

The interconnections between various void regions – geometry effects – are always a problem in adsorption studies. The excellent stepped ^{4}He isotherms of fig. 5 are evidence that our surfaces are far more uniform than Grafoil. Yet the gas relaxation times are quite slow which indicates that adsorption chambers are *not* well connected. We cannot say how this affects the onset properties but remark that this problem is being approached theoretically [27].

Finally, we strongly suspect that the onset contiguity is closely related to the formation of discrete layers in the ZYX film. We have seen that excellent layering features exist for up to 4 complete layers (fig. 5) and a previous ZYX publication indicates liquid formation for thicker films [16]. A vapor pressure study of the growth of ^{4}He films on graphite and other substrates has just been completed [28]. It finds uniform layer deposition up to a critical thickness of about 4 layers and bulk condensation thereafter. The crossover, then, from bulk to uniform film occurs just where our contiguity in onsets appears! It is not entirely clear that the contiguity is a feature of the uniform film rather than merely a peculiarity of vapor flow and droplet location in the ZYX chambers. Although interesting interpretations abound, we prefer not to speculate further at this time.

3.4. Recent developments

Just prior to submission of this manuscript we received preprints reporting new neutron scattering studies of multilayer helium films on graphite. Although performed on Graphon, which possesses poorer homogeneity than either Grafoil or ZYX, pertinent results were obtained. Carneiro et al. [29] confirm earlier heat

capacity evidence for *2nd layer solidification* upon addition of a partial 3rd helium layer [30]. They find a triangular packed solid at a density of 0.092/Å^2, versus 0.115/Å^2 for the monolayer. (Close comparisons of these layer densities with the layer capacities obtained from pressure isotherms can be misleading since underlayer compression occurs and multilayer adsorption areas are not known precisely.)

A second investigation followed the bulk roton integrated scattering intensity and inverse line width from 25 to 4 total helium layers [31]. Both features are linear with coverage and extrapolate to zero in the neighborhood of 3 total atomic layers, of which 2 are solid. These observations are in good agreement with our thermal conductivity irregularity and the vapor pressure estimates of bulk condensation beyond 3–4 atomic layers [27]. The scattering data seem sensitive only to the average film thickness and thus do not provide further evidence regarding the droplet nucleation model [12].

4. Summary

We have taken helium film thermal resistivity and vapor isotherm data on UCAR-ZYX. The film chemical potential shows excellent step features up to 4 complete layers while evidence exists that thicker films are quasi-bulk in character. Film thermal resistances were measured at five temperatures in the range 1.0–1.8 K and their features interpreted in conjunction with the droplet clustering model. Superfluid film onsets on ZYX were compared with those on Grafoil and glass, all of which are compatible with the droplet model of Huberman and Dash.

An irregularity was found in the onset temperature–coverage relation. We associate this feature with the crossover from quasi-bulk (droplet) behavior to distinctly layered films. Comparison with the 2D vortex pair breaking theories is not possible as we have no measurement of superfluid fractions. The thermal resistivity data at 1.0 K involve a film of $2\frac{1}{2}$–$3\frac{1}{3}$ atomic layers, 2 of which are solid! This film is undoubtedly the nearest anyone has yet come to a well-characterized single active layer superfluid helium film.

Acknowledgements

This project was supported by grants from the NSF (DMR 76-20369) and the Rackham Graduate School. We are indebted to J.G. Dash for several excellent suggestions during his careful readings of the manuscript. Discussions with V.K. Wong on the liquid drop model were most valuable. We also thank D.N. Bittner for providing technical assistance throughout this project.

References

[1] K. Fokkens, K.W. Taconis and R. de Bruyn Ouboter, Physica 32 (1966) 2129;
D.F. Brewer and K. Mendelsson, Proc. Roy. Soc. (London) A260 (1961) 1;
E. Long and L. Meyer, Phys. Rev. 85 (1952) 1030; 98 (1955) 1616.

[2] R.S. Kagiwada, J.C. Fraser, I. Rudnick and D. Bergman, Phys. Rev. Letters 22 (1969) 338.

[3] M.H.W. Chan. A.W. Yanof and J.D. Reppy, Phys. Rev. Letters 32 (1974) 1347;
R.P. Henkel, G. Kukich and J.D. Reppy, 11th Conf. on Low Temperature Physics – LT11, St. Andrews, Scotland, UK, 1968.

[4] M. Chester and L.C. Yang, Phys. Rev. Letters 31 (1973) 1377.

[5] Grafoil and ZYX are exfoliates of natural crystal and highly ordered pyrolytic graphite (HOPG) respectively. They are manufactured by the Union Carbide Corp., Carbon Products Div., 270 Park Ave., New York, NY.

[6] J.G. Dash, Films on Solid Surfaces (Academic Press, New York, 1975).

[7] J.M. Kosterlitz and D.J. Thouless, J. Phys. C6 (1973) 1181;
see also D.K. Nelson and J.M. Kosterlitz, Phys. Rev. Letters 39 (1977) 1201.

[8] D.J. Bishop and J.D. Reppy, Phys. Rev. Letters 40 (1978) 1727; J. Physique C6 (1978) 339.

[9] I. Rudnick, Phys. Rev. Letters 40 (1978) 1454.

[10] J.G. Dash, Phys. Rev. Letters 41 (1978) 1178.

[11] S.E. Polanco and M. Bretz, Phys. Rev. B17 (1978) 151.

[12] B.A. Huberman and J.G. Dash, Phys. Rev. B17 (1978) 398.

[13] S.E. Polanco, Ph.D. Thesis, Univ. of Michigan (1979) (unpublished). Available through University Microfilms, Ann Arbor, MI.

[14] M. Bretz, Phys. Rev. Letters 38 (1977) 501.

[15] P.M. Horn, R.J. Birgeneau, P. Heiney and E.M. Hammonds, Phys. Rev. Letters 41 (1978) 961.

[16] S.E. Polanco, J.H. Quateman and M. Bretz, J. Phys. C6 (1978) 344.

[17] If the sponginess of the ZYX is discounted, then Polanco (ref. [13]) estimates that a 4 μm gap will appear between the wafer and cell walls.

[18] There is in principle an additional contribution due to vapor phase conduction. However, since it was calculated to be less than 5% of the empty cell contribution *no* correction was made. See ref. [13] for details.

[19] M. Bretz, Phys. Rev. Letters 31 (1973) 1447.

[20] J.A. Herb and J.G. Dash, Phys. Rev. Letters 29 (1972) 1846.

[21] G. Vidali, M.W. Cole and C. Schwartz, Surface Sci. 87 (1979) L273.

[22] E.S. Sabisky and C.H. Anderson, Phys. Rev. Letters 30 (1973) 1122; Phys. Rev. A7 (1973) 790.

[23] P.K. Hanema and J.R. Kirtley, J. Appl. Phys. 45 (1974) 4016.

[24] M.W. Cole, J.G. Dash and J.A. Herb, Phys. Rev. B11 (1975) 163.

[25] J.G. Dash, Phys. Rev. B15 (1977) 3136.

[26] G.J. Jelatis, J.A. Roth and J.D. Maynard, to be published.

[27] D.A. Huse and R.A. Guyer, to be published;
D.A. Huse and R.A. Guyer, private communication.

[28] M. Bienfait, J.G. Dash and J. Stoltenberg, to be published.

[29] K. Carneiro, L. Passell and W. Thomlinson, to be published;
also J.H. Lauter and H. Wiechert, private communication.

[30] M. Bretz, in: Monolayer and Sub-Monolayer Helium Films, Eds. J.G. Daunt and E. Lerner (Plenum, New York, 1973).

[31] W. Thomlinson, J.A. Tarvin and L. Passell, to be published.